A new radial basis function for Helmholtz problems

J. Lin[a,b], W. Chen[b*], K.Y. Sze[a]

[a] *Department of Mechanical Engineering, The University of Hong Kong, Pokfulam, Hong Kong SAR, P.R.China*
[b] *College of Mechanics and Materials, Hohai University, Nanjing, P.R.China*

Abstract

In this paper, a new radial basis function (RBF) is proposed to solve Helmholtz problems in the traditional collocation method. Since the matrix equation arising from the RBF interpolation is ill-conditioned, a regularized singular value decomposition method is used to obtain a more accurate solution. Numerical examples of both direct and inverse problems are presented to demonstrate the effectiveness and applicability of the proposed RBF versus the traditional multiquadric RBF.

Key words: radial basis function; regularization technique; Helmholtz problem

1. Introduction

A large variety of RBFs or RBF-based methods have been proposed. Commonly-used RBFs, such as multiquadric (MQ) [1, 2], inverse multiquadric [3], and thin plate spline [4, 5], have been widely studied. The popular RBF-based numerical methods include the method of fundamental solutions (MFS) [6, 7], boundary collocation method [8, 9], regularized meshless method [10, 11], radial basis function networks [12, 13], radial basis collocation method [14, 15], boundary distributed source method [16], and boundary knot method (BKM) [17, 18], etc. In the past several decades, the above RBFs or RBF-based methods have been applied to solve heat transfer problems [19, 20], 1D and 2D nonlinear Burgers' equation [21, 22], shallow water equation for tide and currents simulation [23], harmonic elastic and viscoelastic problems [24], among others.

*Corresponding author: chenwen@hhu.edu.cn
Published in Engineering Analysis with Boundary Elements 36 (2012) 1923–1930
http://dx.doi.org/10.1016/j.enganabound.2012.07.010

The initial development of applying RBFs to solve partial differential equation began from the pioneering work of Kansa [25, 26], named as Kansa's method. In this method, RBFs are directly used as the basis to approximate the solutions by enforcing the governing equation and boundary conditions on collocation points. The MQ was first developed by Hardy [27] as a multi-dimensional scattered interpolation in approximating the gravitational field of the earth. It was not recognized by most of the researchers until Franke [28] published a paper in which the accuracy, efficiency, storage, and the ease of implementation of 29 interpolation methods were evaluated and MQ was ranked as the overall best. When applying some RBF-based methods, such as the MFS and BKM, to non-homogeneous problems [29, 30], one needs to resort to a two-step method. That is to say, one should first approximate the particular solution by dual reciprocity method or other methodologies, and then derive the general solution for the corresponding homogeneous problems. Compared with these numerical methods, the radial basis collocation method [31, 32, 33, 34] is a single-step method for both homogeneous and non-homogeneous problems. However, the accuracy of the method is highly sensitive to the choice of RBF.

In this study, a new RBF to be used in the radial basis collocation method is proposed for the both direct and inverse Helmholtz problems. It is based on the general solution of Helmholtz equation. This type of RBF is constructed by a heuristic approach without rigorous mathematical analysis. To illustrate its effectiveness and efficiency, several direct and inverse problems are considered. In the direct problems, the coefficient matrix generated by the new RBF is often ill-conditioned as those generated by other traditional RBFs [35, 36]. In the inverse problems, we only consider the classical Cauchy problems in which boundary conditions for both the solution and its normal derivative are prescribed only on a portion of the boundary, whilst no information is available on the remaining part. So, we should reconstruct the solution on the unaccessible boundary and in the domain. The Cauchy problem is much more difficult to solve both analytically and numerically than the direct problem, since the solution does not satisfy the general conditions of well-posedness. The solution is not a continuous function of the boundary data and a small error in the accessible data may result in an enormous error in the numerical solution, this kind of problem is ill-posed [37]. We can not use direct approach, such as the Gauss elimination method, in order to solve the system of linear equations which arises from the discretisation of the problem. To handle ill-conditioned or ill-posed problems, many reg-

ularization techniques have been adopted [37, 38, 39]. Here, we extend the new RBF combined with the damped singular value decomposition (DSVD) regularization technique to Cauchy problems. The generalized cross validation (GCV) [37] is one of strategies to estimate an appropriate regularization parameter of the DSVD and is employed in our numerical experiments.

The rest of the paper is organized as follows. In Section 2, formulations of the direct and inverse problems are briefly reviewed whereas the new RBF would be introduced. The DSVD under parameter choice of GCV is described in Section 3. In Section 4, four numerical examples are employed to study the accuracy, efficiency, convergence and the numerical conditioning of or related to the new RBF. Section 5 concludes this study with some remarks.

2. Problem description and the new radial basis function

2.1. Direct and inverse problems

We consider the following non-homogeneous Helmholtz equation

$$\nabla^2 u(x,y) + k^2 u(x,y) = f(x,y), \qquad \text{in } \Omega, \tag{1}$$

where ∇^2 is the Laplacian, k the wave-number, Ω represents a simply connected domain in R^2, and $f(x,y)$ is the source term.

For direct problems under investigation require solving equation (1) subjected to the following boundary conditions

$$u(x,y) = g(x,y), \qquad \text{on } \Gamma_1, \tag{2}$$

$$\frac{\partial u(x,y)}{\partial n} = h(x,y), \qquad \text{on } \Gamma_2, \tag{3}$$

where $\Gamma_1 \cap \Gamma_2 = \phi$ and $\Gamma_1 \cup \Gamma_2 = \partial\Omega$, $\partial u/\partial n$ denotes the outward normal derivative of u. Lastly, $g(x,y)$ and $h(x,y)$ are the measured Dirichlet and Neumann data on boundaries Γ_1 and Γ_2, respectively.

For Cauchy problems, the boundary condition is not known on the whole boundary $\partial\Omega$

$$u(x,y) = g(x,y), \qquad \text{on } \Gamma_1, \tag{4}$$

where Γ_1 is the accessible part of the boundary $\partial\Omega$. The governing equation (1) subjected to only the boundary condition (4) is mathematically underdetermined, and additional data must be supplied to fully determine it. The

additional data available is given by a boundary condition different from that given by equation (4),

$$\frac{\partial u(x,y)}{\partial n} = h(x,y), \qquad \text{on } \Gamma_1. \tag{5}$$

Note that in this case, the accessible part of the boundary Γ_1 is overspecified, since two different types of boundary conditions are prescribed on it. A necessary condition for the above Cauchy problem (1),(4) and (5) to be identifiable is that the known boundary part Γ_1 is larger than the under-specified boundary part $\Gamma_2 = \partial\Omega/\Gamma_1$. And in this study, we focus on determining the underprescribed functions on the inaccessible boundary Γ_2 and in the solution domain.

2.2. The new radial basis function

At first, general solution of equation (1) is as follows:

$$\varphi(\mathbf{x}, \mathbf{x}_j) = J_0(kr), \tag{6}$$

where J_0 denotes the zero-th order Bessel function of the first kind, $r = r(\mathbf{x}, \mathbf{x}_j)$ is the Euclidian distance between the general points $\mathbf{x} = (x, y)$ and the origin of the RBF $\mathbf{x}_j = (x_j, y_j)$, k the wave-number. In order to solve the nonhomogeneous problem, we propose the following radial basis function:

$$\varphi(\mathbf{x}, \mathbf{x}_j) = J_0(k(r^2 + C^2)^{1/2}), \tag{7}$$

where C is an empirically chosen shape parameter. It can be seen that the well-known MQ function $(r^2(\mathbf{x}, \mathbf{x}_j)+C^2)^{1/2})$ is an argument of this new RBF. The approximation solution is expressed by linear combination of the new RBF (7),

$$u_N(\mathbf{x}) = \sum_{j=1}^{N} \alpha_j \varphi(\mathbf{x}, \mathbf{x}_j) \tag{8}$$

where α_j is the unknown coefficient to be determined. In our computations, the collocation points to enforce the governing equation or the boundary conditions are identical to the RBF origins. We use $\{x_j\}_1^{N_I}$, $\{x_j\}_{N_I+1}^{N_I+N_D}$ and $\{x_j\}_{N_I+N_D+1}^{N}$ to denote the collocation points in Ω, on Γ_1 and on Γ_2, respec-

tively. Hence, the following linear algebraic equations on α_js are resulted:

$$\sum_{j=1}^{N} \alpha_j (\nabla^2 \varphi(\mathbf{x}_i, \mathbf{x}_j) + k^2 \varphi(\mathbf{x}_i, \mathbf{x}_j)) = f(\mathbf{x}_i),\ i = 1, 2, \ldots, N_I \tag{9}$$

$$\sum_{j=1}^{N} \alpha_j \varphi(\mathbf{x}_i, \mathbf{x}_j) = g(\mathbf{x}_i),\ i = N_I + 1, \ldots, N_I + N_D \tag{10}$$

$$\sum_{j=1}^{N} \alpha_j \frac{\partial \varphi(\mathbf{x}_i, \mathbf{x}_j)}{\partial n} = h(\mathbf{x}_i),\ i = N_I + N_D + 1, \ldots, N \tag{11}$$

which can be written in the following matrix form:

$$[A_{ij}][\alpha_j] = [b_i] \tag{12}$$

The coefficients matrix $[A_{ij}]$ is often ill-conditioned for both direct and inverse problems. With an ill-conditioned matrix, the predictions would be unstable especially when the input data contains noise [37]. In this context, regularization methods have been used to remedy the instability and accuracy loss in the solution of ill-conditioned matrix equations [37, 40, 41]. In this paper, we shall employ the DSVD under parameter choice of GCV which is introduced in the following section.

3. Regularization method and regularization parameter

Before presenting the regularization method and regularization parameter, we introduce the singular value decomposition (SVD) of the coefficient matrix in (12),

$$A = W \Sigma V^T \tag{13}$$

where $W = [w_1, w_2, \cdots, w_N] \in R^{N \times N}$, $W^T W = I_N$ and $V = [v_1, v_2, \cdots, v_N] \in R^{N \times N}$, $V^T V = I_N$ and I_N denotes the N-th order identity matrix. The singular values of A are the diagonal entries of $\Sigma = \text{diag}(\sigma_1, \sigma_2, \cdots, \sigma_N)$ which has non-negative diagonal elements appearing in non-increasing order such that

$$\sigma_1 \geq \sigma_2 \geq \cdots \geq \sigma_N \geq 0, \tag{14}$$

The column vectors w_i and v_i are, respectively, left- and right-singular vectors for the corresponding singular values. Using the SVD, it is easy to get the

solution to (12)

$$\alpha = \sum_{i=1}^{N} \frac{w_i^T b v_i}{\sigma_i}. \tag{15}$$

Remark: The conventional L_2 condition number of A is defined as $\mathrm{Cond}(A) = \sigma_1/\sigma_N$, in which σ_1 and σ_N are the largest and smallest singular values of A.

3.1. Regularization Method

The Damped Singular Value Decomposition (DSVD) is based on the SVD and the Tikhonov regularization technique (TR) [37]. The idea of TR is to define the regularized solution to (12) by the following penalized least-squares problem

$$\min\{\| A\alpha - b \|_2^2 + \xi^2 \| I\alpha \|_2^2\} \tag{16}$$

In the expression, $\| \, . \, \|_2$ denotes the Euclidean norm and ξ is the regularization parameter which controls the relative weight of the penalty term.

Based on the SVD, the TR solution can be expressed as

$$\alpha = \sum_{i=1}^{N} g_i \frac{w_i^T b v_i}{\sigma_i}, \tag{17}$$

where the Wiener weights g_is are:

$$g_i = \frac{\sigma_i^2}{\sigma_i^2 + \xi^2}. \tag{18}$$

Here, instead of using the filter factors (18) in the TR, one introduces a smoother cut-off by means of filter factor g_i defined as

$$g_i = \frac{\sigma_i}{\sigma_i + \xi}. \tag{19}$$

This filter factor decays less slowly than the Tikhonov filter factor, and thus, in a sense, introduces less filtering. The performance of regularization method depends to a great extent on the suitable choice of the regularization parameter. In this paper, we use the generalized cross validation method to provide appropriate regularization parameter.

3.2. Regularization Parameter

The Generalized Cross Validation (GCV) estimates the optimal value of the regularization parameter by minimizing

$$V(\alpha) = \frac{\frac{1}{N}\|(I - B(\alpha))b\|_2^2}{[\frac{1}{N}\text{trace}(I - B(\alpha))]^2}, \tag{20}$$

where the influence matrix $B(k)$ is defined by the identity

$$Ba_\alpha = B(\alpha)b. \tag{21}$$

The GCV has some computationally relevant properties. Moreover, it is a predictive mean-square error criterion, in the sense that it estimates the minimizer of the residual function

$$T(K) = \frac{1}{N}\|B(\alpha_K - \alpha)\|_2^2. \tag{22}$$

Here, it is noted that, in the following numerical studies, we do not have to use the regularization method for the direct problem. For Cauchy problems, we use the above-mentioned DSVD under the parameter choice of GCV procedure to solve such ill-conditioned or ill-posed systems.

4. Numerical results and discussions

For both direct and inverse problems, several numerical examples are studied from which the accuracy and stability of the proposed RBF are illustrated. The relative average error (L_2 relative error) to be shown in the subsequent figures is defined as:

$$\text{Relative average error} = \sqrt{\frac{\sum_{j=1}^{N_t}\left(u(x_j, y_j) - \tilde{u}(x_j, y_j)\right)^2}{\sum_{j=1}^{N_t}(u(x_j, y_j))^2}}$$

where (x_j, y_j) denotes the j-th test point, N_t is the total number of tested points, u is the exact solution, $\tilde{u}$ is the numerical prediction. In particular, the MATLAB regularization code developed by Hansen is used in our computations [42].

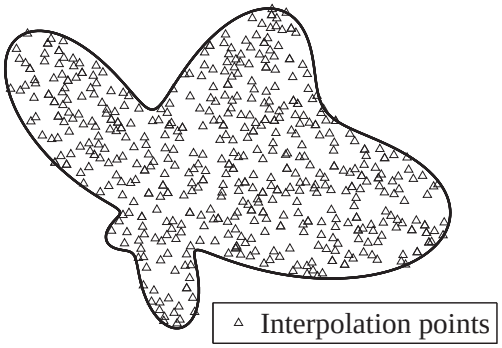

Figure 1: Amoeba-shaped domain.

4.1. Direct Helmholtz problems in an amoeba-shaped domain

In this example, a Dirichlet Helmholtz direct problem with non-zero source term is considered, and the corresponding exact solution and source term are

$$u(x,y) = \sin(kx)\sinh(y)+\cos(y) \quad , \quad f(x,y) = \sin(kx)\sinh(y)-\cos(y)+k^2 cos(y) \tag{23}$$

In this case, we choose the wave-number $k = 10$. The amoeba-shaped domain as shown in Figure 1 is bounded by the following parametric equation:

$$\partial\Omega = \{(x,y)\,|x = \rho\cos\theta, y = \rho\sin\theta, 0 \leq \theta \leq 2\pi\}\,, \tag{24}$$

where

$$\rho = e^{\sin(\theta)}\sin^2(2\theta) + e^{\cos(\theta)}\cos^2(2\theta). \tag{25}$$

Collocation points randomly-distributed inside the domain and on the boundary are placed in a comparative study of the MQ and present new RBF. The relative average errors of the MQ and new RBF versus the shape parameter C are plotted in Figure 2. The MQ is less accurate and its convergence curve is more sensitive to shape parameter C.

Generally speaking, the error of MQ deceases as shape parameter C increases with a fixed number of collocation points and then starts to deteriorate after an optimal value of C. It is noted that the MQ has a smoother error curve than the new RBF.

Figure 3 shows the condition numbers of the coefficient matrices of the

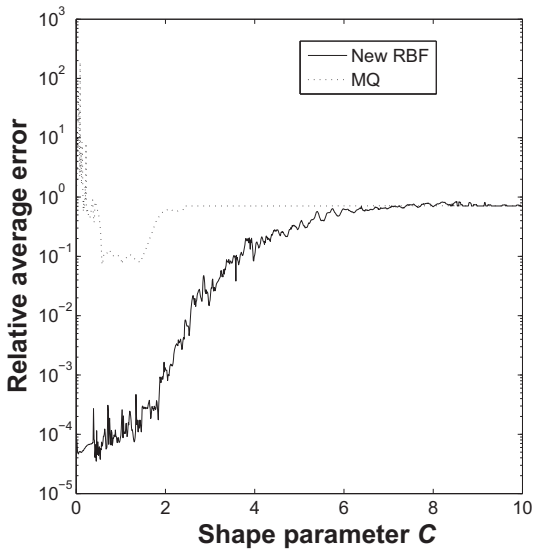

Figure 2: Error analysis with different shape parameters C with $N = 405$ collocation points and 205 inner interpolation points.

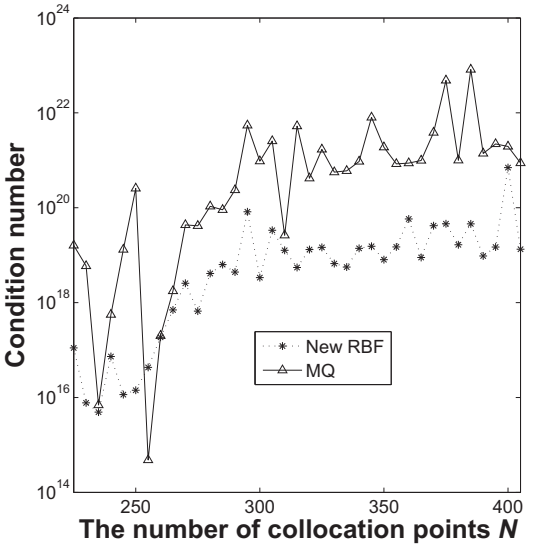

Figure 3: Condition numbers versus the number of collocation points N with optimal C and 205 inner interpolation points.

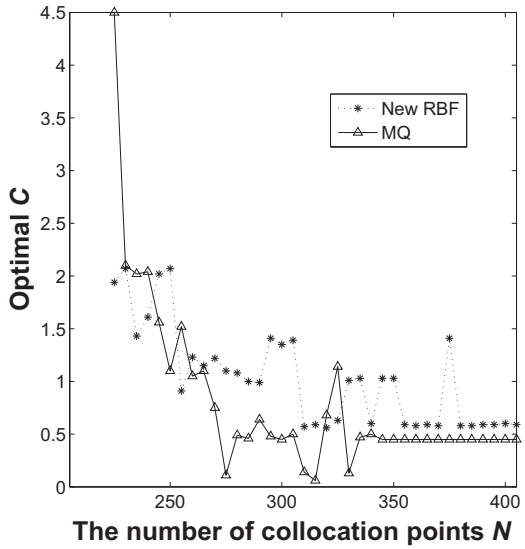

Figure 4: Optimal C versus the number of collocation points N.

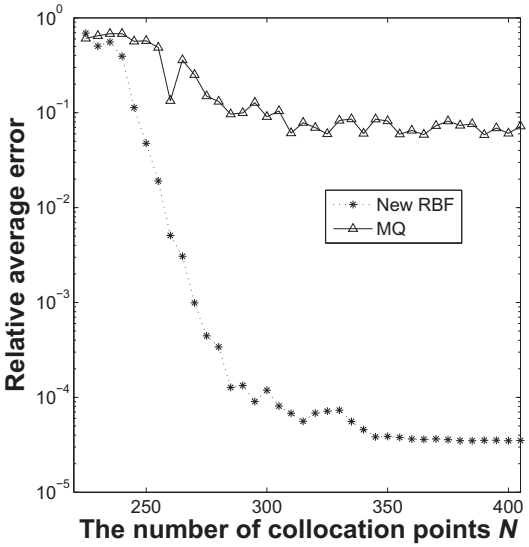

Figure 5: Relative average errors versus the number of collocation points N with optimal C.

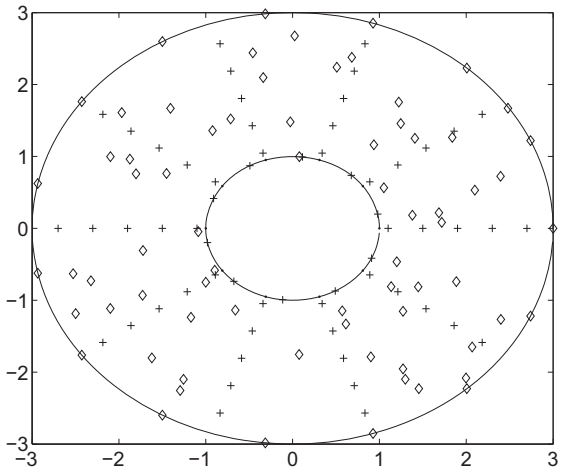

Figure 6: Typical distributions of collocation points ("+" in Ω, "$\times$" and "." on Γ_1) and test points "$\diamondsuit$" in the annular with radii 1 and 3.

MQ and new RBF versus the number of collocation points with optimal shape parameter C. They all result in severely ill-conditioned matrix. For both RBFs, the condition numbers increase sharply with an increasing number of collocation points. It is noted that the optimal shape parameter C varies from 0.001 to 10 based on the known analytical solution. Optimal C against the number of collocation points N is displayed in Figure 4, we can see that the optimal C tends to be smaller for both RBFs due to increasing density of collocation points.

Convergence is shown in Figure 5 in which the relative average errors are plotted against the number of collocation points for the optimal C. Results by both RBFs converge very fast regarding the number of collocation points. The relative average error of MQ is around 10^{-1}, while the errors of the new RBF becomes steady at 10^{-5}, with large number of collocation points N. It is clearly seen that the new RBF has higher accuracy than the MQ.

4.2. Inverse Helmholtz problems for an annular domain

In this section, the inverse Helmholtz problem with the following exact solution and source term is considered:

$$u(x, y) = \sin(x) + \sin(y) + x \quad , \quad f(x, y) = x \tag{26}$$

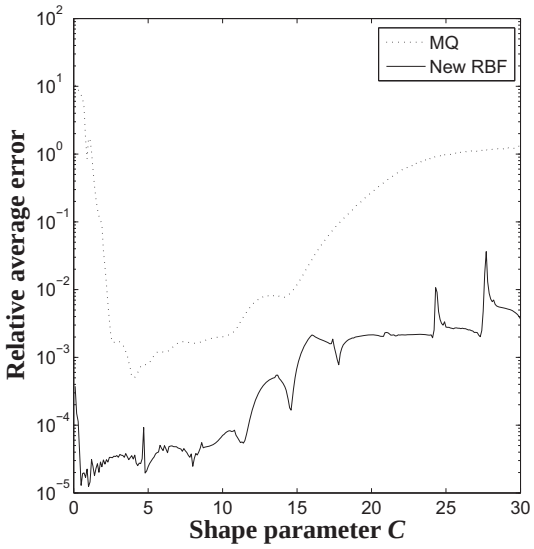

Figure 7: Relative average errors versus the shape parameters C in the case of annular domain with $N = 225$ collocation points.

The domain $\Omega = \{(x, y)|1 \leq \sqrt{(x^2 + y^2)} \leq 3\}$ with both the Dirichlet and Neumann boundary conditions known simultaneously on the inner boundary $\Gamma_1 = \{(x, y)|(x^2 + y^2) = 1\}$. A typical distribution of the collocation and sampling points are shown in Figure 6. we are looking for the boundary condition in the outside boundary $\Gamma_2 = \{(x, y)|\sqrt{x^2 + y^2} = 3\}$ and solution in the domain. Here, we choose randomly distributed 360 knots in the domain and 100 knots on the boundary Γ_2 as the test knots in Figures 7-9.

The relative average errors versus the shape parameter C are shown in Figure 7 with the invariant number of collocation points $N = 225$. Compared with the new RBF, the MQ is less accurate and its accuracy depends strongly on the choice of C. Moreover, the relative average error of MQ can exceed 10 with an inappropriate choice of the shape parameter C.

For the new RBF, the relative average error starts around 5×10^{-3} for small C and becomes rather steady at 5×10^{-4} when C is less than 10. With increased value of C, less accurate results are obtained for both RBFs. We observe the similar behavior pattern between the accuracy and the shape parameter C for a large collocation point number N.

The contours of the absolute errors produced by the MQ and the new RBF with $C = 2$ and $N = 225$ are plotted in Figure 8. From the numerical

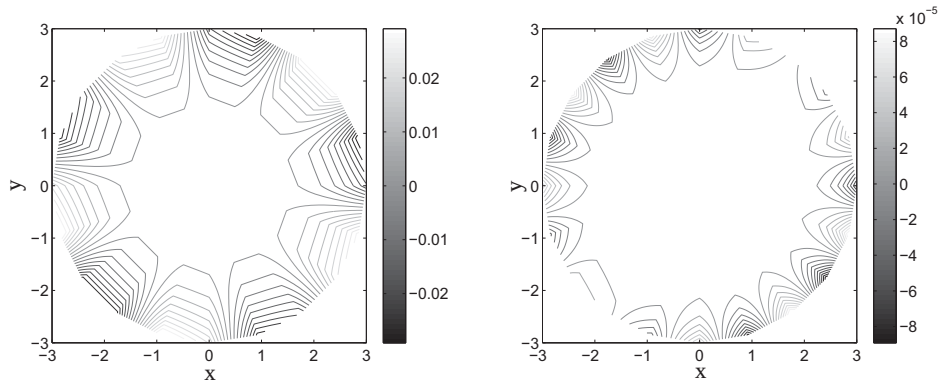

Figure 8: Contour of the absolute errors: MQ (left) and the new RBF (right) for the annular domain with $C = 2, N = 225$.

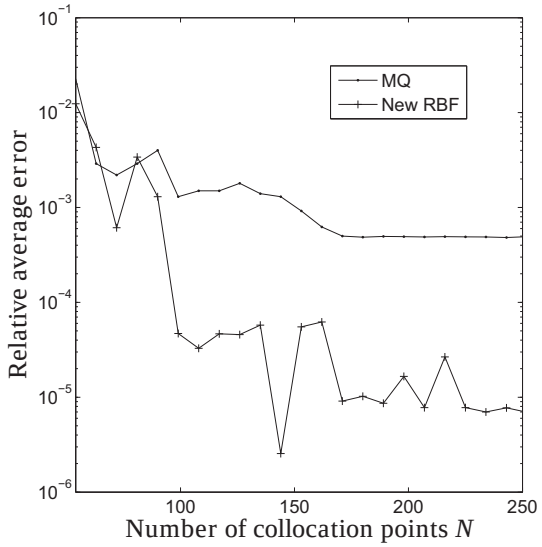

Figure 9: Relative average errors versus the number of collocation points N in the case of annular domain with optimal C.

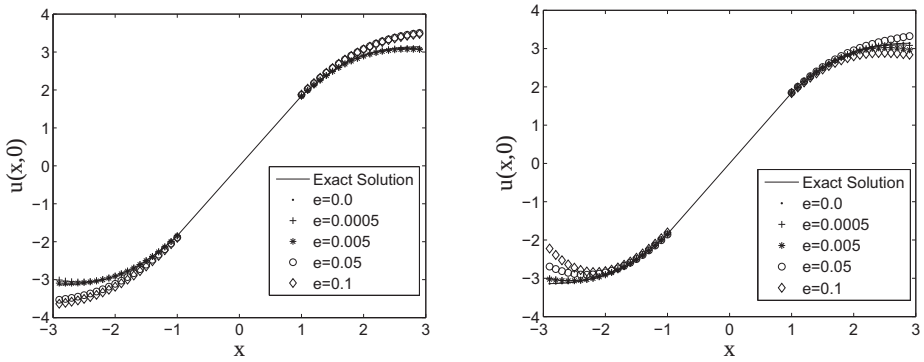

Figure 10: Recovery of u(x,0) by MQ (left) and new RBF (right) at different noise levels.

predictions, the error of MQ varies between -3.22×10^{-2} and 3.22×10^{-2} whereas the error of the new RBF varies between -9.84×10^{-5} and 9.64×10^{-5}. And Figure 9 profiles that the new RBF is 10^2 times more accurate than MQ for large N. It is noted that in Figure 9, we take the optimal shape parameter C for each number of collocation points N for both RBFs.

Considering that there are always some errors for the observation data in real applications. The boundary data on Γ_1 are taken to be

$$g(x,y) = u(x,y)(1 + e \cdot noise) \quad , \quad h(x,y) = \frac{\partial u(x,y)}{\partial n}(1 + e \cdot noise) \quad (27)$$

where $noise = -1 + 2 \cdot \text{Rand}$, e is the noise level and Rand is the MATLAB function which generates uniformly distributed-random numbers between 0 and 1.

The recovered $u(x,0)$ and $u(0,y)$ using the two RBFs at different noise levels are plotted in Figure 10. The results show that when e <0.05, the solutions of both RBFs agree very well with the exact one. When e goes up to 0.05, solution deteriorations can be noted for both RBFs.

4.3. Inverse Helmholtz problems for a square domain

For the present inverse problem, the exact solution and the source term are:

$$u(x,y) = sin(\sqrt{3}x)sinh(y) + cos(\sqrt{2}y) + x - 2y \quad , \quad f(x,y) = 2x - 4y \quad (28)$$

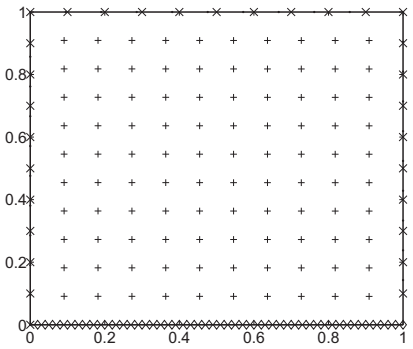

Figure 11: Typical distributions of collocation points ("+" in Ω, "$\times$" on Γ_1, "." on Γ_2) and test points "$\diamondsuit$" for unit square.

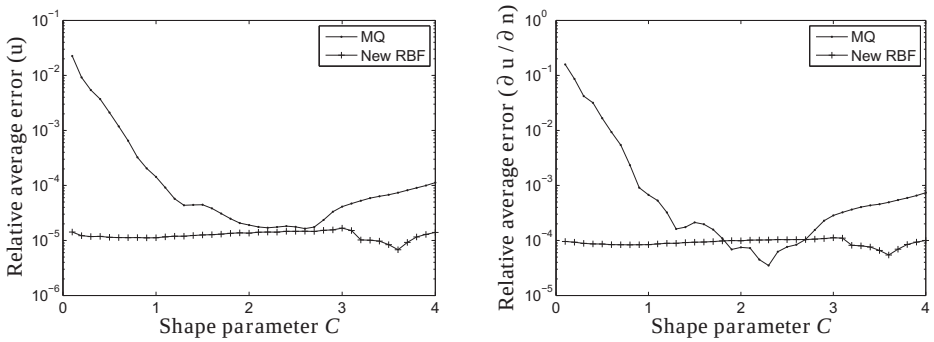

Figure 12: Relative average errors of u (left) and $\partial u/\partial n$ (right) versus shape parameters C for unit square with the number of collocation points $N = 160$.

Moreover, $\Omega = \{(x, y) \mid 0 \leqslant x \leqslant 1, 0 \leqslant y \leqslant 1\}$, $\Gamma_2 = \{(x, 0) \mid 0 \leqslant x \leqslant 1\}$ and $\Gamma_1 = \partial\Omega \backslash \Gamma_2$.

A typical distribution of the collocation and sampling points are portrayed in Figure 11.

The relative average errors of the recovered u and $\partial u/\partial n$ on Γ_2 with different shape parameters C ($N = 160$) are shown in Figure 12. It can be seen that the errors of MQ are considerably more sensitive to the choice of C than the new RBF. The latter is more accurate than the former nearly over the entire range of C.

The solution convergence is shown in Figure 13. It illustrates that the relative average errors of the new RBF decreases more quickly than MQ when

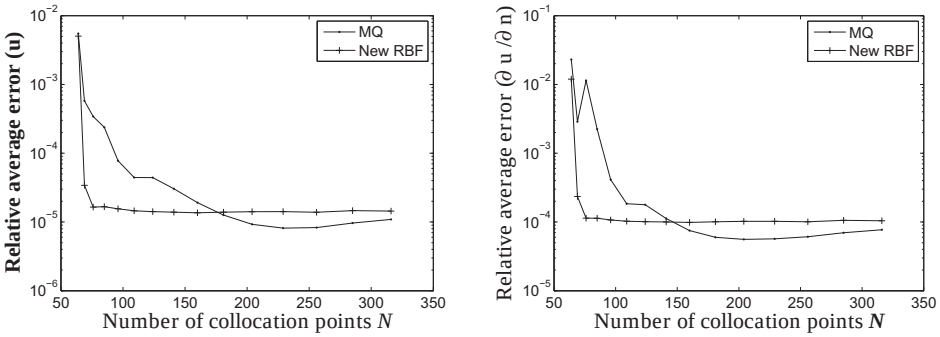

Figure 13: Relative average errors of u (left) and $\partial u/\partial n$ (right) versus the number of collocation points N for unit square.

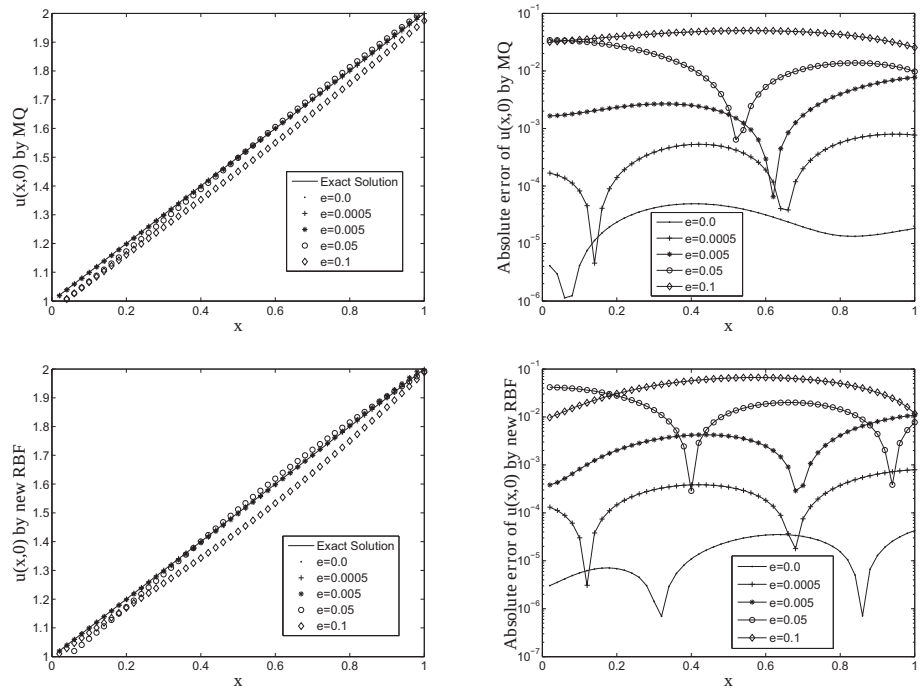

Figure 14: Recovery of the u(x,0) by MQ (up) and the new RBF (down) at different noise levels.

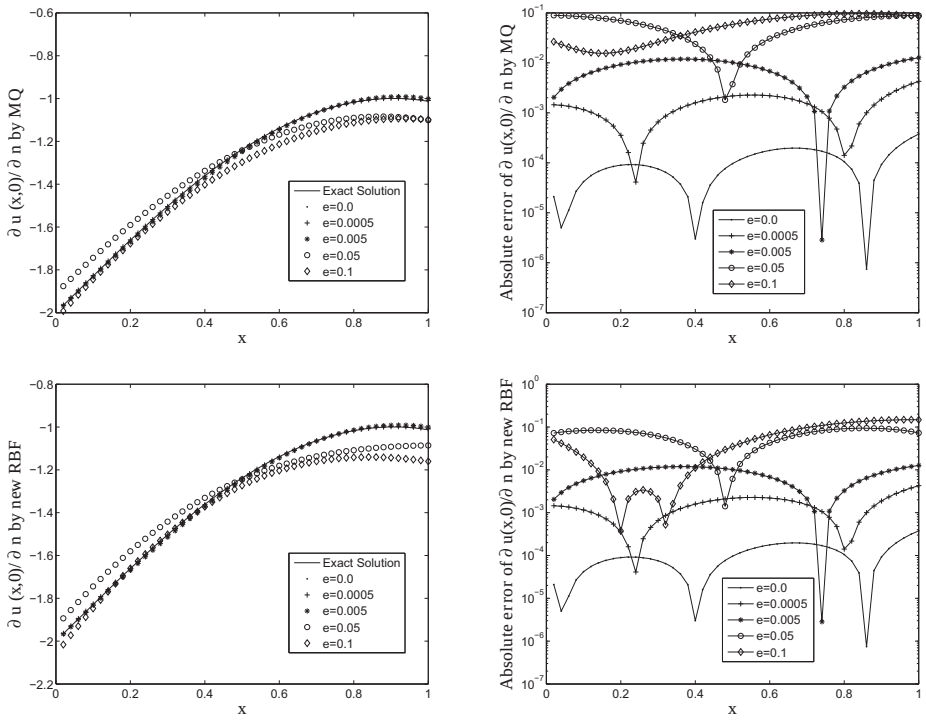

Figure 15: Recovery of the ∂u(x,0) / ∂n by MQ (up) and the new RBF (down) at different noise levels.

$N < 76$. The errors of both RBFs are rather stable when $N > 229$. Similar results are shown for $\partial u/\partial n$ in Figure 13 (right). The results in Figure 13 are obtained by $C = 2$.

In order to test the sensitivity of the solutions to the input data noise, the same input data in Section 4.2 for $g(x, y)$ and $h(x, y)$ is used. The recovered u and $\partial u/\partial n$ by both RBFs are shown in Figures 14 and 15 for various noise levels and, again, $C = 2$ is employed. We can see that the approximate solution u calculated by both RBFs agree very well with the exact solution up to the noise level $e = 0.05$, and then, deteriorate with a larger noise level e. It is worthy of noting that the new RBF produces 10 times more accurate approximate solution u than the MQ in the case of non-noise boundary data. For $\partial u/\partial n$, both RBFs, however, have almost the same accuracy with non-noisy boundary data. And for moderate noise ($e \leq 0.005$), acceptable approximate $\partial u/\partial n$ can also be obtained by both RBFs.

5. Concluding remarks

In this paper, a new radial basis function is proposed for both the direct and inverse Helmholtz boundary value problems. Regularization technique is employed to tackle the ill-conditioned direct problems and ill-posed inverse problems. It can be seen from the three benchmark examples in Section 4 that reasonable solutions can be obtained by the proposed RBF in both direct problems and inverse problems with and without noisy boundary data for a wide range of shape parameter.

Despite of the excellent performance in scattered data approximation, the traditional MQ fails to yield acceptable numerical solutions unless shape parameter C is optimally chosen.

Acknowledgement

The work described in this paper was supported by National Basic Research Program of China (973 Project No. 2010CB832702), the Opening Fund of the State Key Laboratory of Structural Analysis for Industrial Equipment (GZ0902), and the R&D Special Fund for Public Welfare Industry (Hydrodynamics, Project No. 201101014). The first author thanks the Jiangsu Province Graduate Students Research and Innovation Plan (Project No. CXZZ12_0226).

References

[1] A.H.-D. Cheng, M.A. Golberg, E.J. Kansa and G. Zammito, Exponential convergence and *H-c* multiquadric collocation method for partial differential equations, *Numerical Methods for Partial Differential Equations*, 19 (2003) 571-594.

[2] E.J. Kansa, Multiquadrics-A scattered data approximation scheme with applications to computational fluid-dynamics-I surface approximations and partial derivative estimates , *Computers & Mathematics with Applications*, 19 (1990) 127-145.

[3] X.G. Hu, T.S. Ho and H. Rabitz, The collocation method based on a generalized inverse multiquadric basis for bound-state problems, *Computer Physics Communications*, 112 (1998) 168-179.

[4] A.C. Faul and M.J.D. Powell, Proof of convergence of an iterative technique for thin plate spline interpolation in two dimensions, *Advances in Computational Mathematics*, 11 (1999) 193-192.

[5] M.J.D. Powell, The uniform convergence of thin plate spline interpolation in two dimensions, *Numerische Mathematik*, 68 (1994) 107-128.

[6] G. Fairweather, A. Karageorghis, The method of fundamental solutions for elliptic boundary value problems, *Advances in Computational Mathematics*, 9 (1998) 69-95.

[7] M.A. Golberg, C.S. Chen, *The method of fundamental solutions for potential, Helmholtz and diffusion problems, in: M.A. Golberg (Eds.), Boundary inetgral methods: numerical and mathematical aspects*, Computational Mechanics Publications, 1998, pp.103-176.

[8] J.T. Chen, M.H. Chang, K.H. Chen and S.R. Lin, The boundary collocation method with meshless concept for acoustic eigenanalysis of two-dimension cavities using radial basis function, *Journal of Sound and Vibration*, 257 (2002) 667-711.

[9] J.A. Kolodziej, M. Kleiber, Boundary collocation method vs fem for some harmonic 2-d problems, *Computers & Structures*, 33 (1989) 155-168

[10] D.L. Young, K.H. Chen and C.W. Lee, Novel meshless method for solving the potential problems with arbitrary domain, *Journal of Computational Physics*, 209 (2005) 290-321.

[11] W. Chen, J. Lin, F.Z. Wang. Regularized meshless method for inhomogeneous problems, *Engineering Analysis with Boundary Elements*, 35 (2011) 253-257.

[12] N. Mai-Duy, T. Tran-Cong, A meshless technique based on integrated radial basis function networks for elliptic partial differential equations, *Mathematics And Statistics*, 65 (2008) 141-155.

[13] N. Mai-Duy, T. Tran-Cong, Numerical solution of differential equations using multiquadric radial basis function networks, *Neural Networks*, 14 (2001) 185-199.

[14] H.Y. Hu, Z.C. Li, A.H.-D. Cheng, Radial basis collocation methods for elliptic boundary value problems, *Computers & Mathematics with Applications*, 50 (2005) 289-320.

[15] H.Y. Hu, J.S. Chen and W. Hu, Weighted radial basis collocation method for boundary value problems, *International Journal For Numerical Methods In Engineering*, 69 (2007) 2736-2757.

[16] Y.J. Liu, A new boundary meshfree method with distributed sources, *Engineering Analysis with Boundary Elements*, 34 (2010) 914-919.

[17] B.T. Jin, W. Chen, Boundary knot method based on geodesic distance for anisotropic problems, *Journal of Computational Physics*, 215 (2006) 614-629.

[18] F.Z. Wang, L. Ling, W. Chen, Effective condition number for boundary knot method, *CMC: Computers, Materials, & Continua*, 12 (2009) 57-70.

[19] E. Divo and A. Kassab, An efficient localised radial basis function meshless method for fluid flow and conjugate heat transfer, *Journal of Heat Transfer*, 129 (2007) 124-136.

[20] M. Zerroukat, H. Power, C. S. Chen, A numerical method for heat transfer problems using collocation and radial basis functions, *International Journal For Numerical Methods In Engineering*, 42 (1998) 1263-1278.

[21] J. Li, Y.C. Hon, C.S. Chen, Numerical comparisons of two meshless methods using radial basis functions, *Engineering Analysis with Boundary Elements*, 26 (2002) 205-225.

[22] Y.C. Hon, X.Z. Mao, An efficient numerical scheme for Burgers' equation, *Applied Mathematics and Computation*, 95 (1998) 37-50.

[23] Y.C. Hon, K.F. Cheung, X.Z. Mao, E.J. Kansa, Multiquadric solution for shallow water equations, *Journal of Hydraulic Engineering*, 125 (1999) 524-533.

[24] A. Canelas, B. Sensale, A boundary knot method for harmonic elastic and viscoelastic problems using single-domain approach, *Engineering Analysis with Boundary Elements*, 34 (2010) 845-855.

[25] E.J. Kansa, Multiquadric-a scattered data approximation scheme with applications to computational fluid dynamics II, *Computers & Mathematics with Applications*, 19 (1990) 147-61.

[26] C. Franke, R. Schaback, Solving partial differential equations by collocation using radial basis functions, *Applied Mathematics and Computation*, 93 (1998) 73-82.

[27] R.L. Hardy, Multiquadric equations of topography and other irregular surfaces, *Journal of Geophysical Research*, 76 (1971) 1905-1915.

[28] R. Franke, Scattered data interpolation: tests of some methods, *Mathematics of Computation*, 38 (1982) 181-200.

[29] G.C. de Medeiros, P.W. Partridge, and J.O. Brandao, The method of fundamental solutions with dual reciprocity for some problems in elasticity, *Engineering Analysis with Boundary Elements*, 28 (2004) 453-461.

[30] M.A. Golberg, The method of fundamental solutions for Poisson's equation, *Engineering Analysis with Boundary Elements*, 16 (1995) 205-213.

[31] J.C. Li, C.S. Chen, Some observations on unsymmetric radial basis function collocation methods for convection-diffusion problems, *International Journal for Numerical Methods in Engineering*, 57 (2003) 1085-1094.

[32] B. Šarler, J. Perko and C.S. Chen, Radial basis function collocation method solution of natural convection in porous media, *International Journal of Numerical Methods Heat & Fluid Flow*, 14 (2004) 187-212.

[33] R. Vertnik, B. Šarler, Meshless local radial basis function collocation method for convective-diffusive solid-liquid phase change problems, *International Journal of Numerical Methods for Heat & Fluid Flow*, 16 (2006) 617-640.

[34] C. Franke, R. Schaback, Convergence order estimates of meshless collocation methods using radial basis functions, *Advances in Computional Mathematics*, 8 (1998) 381-399

[35] E.J. Kansa, Y.C. Hon, Circumventing the ill-conditioning problem with multiquadric radial basis functions: Applications to elliptic partial differential equations, *Computers & Mathematics with Applications*, 39 (2000) 123-137.

[36] C.S. Chen, H.A. Cho, M.A. Golberg, Some comments on the ill-conditioning of the method of fundamental solutions, *Engineering Analysis with Boundary Elements*, 30 (2006) 405-410.

[37] T. Wei, Y.C. Hon, L. Ling, Method of fundamental solutions with regularization techniques for Cauchy problems of elliptic operators, *Engineering Analysis with Boundary Elements*, 31 (2007) 373-385.

[38] A.N. Tikhonov, V.Y. Arsenin, Solutions of Ill-Posed Problems, *SIAM Review*, 21 (1979) 266-267.

[39] A.N. Tikhonov, A.V. Goncharsky, V.V. Stepanov and A.G. Yagola, *Numerical Methods for the Solution of Ill-Posed Problems*, Kluwer Academic Publishers, MA, Boston (1995).

[40] F.Z. Wang, W. Chen, X.R. Jiang, Investigation of regularized techniques for boundary knot method, *International Journal for Numerical Methods in Biomedical Engineering*, 26 (2010) 1868-1877.

[41] J. Lin, W. Chen, F.Z. Wang, A new investigation into regularization techniques for the method of fundamental solutions, *Mathematics and Computers in Simulation*, 81 (2011) 1144-1152.

[42] P.C. Hansen, Regularization tools: A Matlab package for analysis and solution of discrete ill-posed problems, *Numerical Algorithms*, 6 (1994) 1-35.